CHAPTER IV
RESULTS AND DISCUSSION

4.1 Study on Properties of Commercial Biodegradable Plastic Bags

4.1.1 Structural Characterization

Figure 4.3 (a) shows an FTIR spectrum of PLA (NatureWorks® 4042D). The small IR bands at 3655 and 3503 cm^{-1} are assigned to the free OH stretching region which belongs to the OH group at the chain end of PLA. The CH_2 repeat unit can be confirmed from the 2995~2880 cm^{-1}. The ester group is shown at 1751 cm^{-1} (C=O stretching). The band at 1456 cm^{-1} is assigned to the CH_3 bending region. The region between 1383 and 1364 cm^{-1} belongs to CH deformation. The C-O stretching bands represent at the region between 1190 and 1090 cm^{-1}.

Here, a series of the commercial products were characterized by FTIR to obtain basic information about the PLA compounding of each product (Figure 4.3). Figure 4.3 (b) shows the FTIR spectrum of poly(butylene succinate adipate) or PBSA (Bionolle® 3001G) (as shown in Figure 4.1). The important peaks are 3430 cm^{-1} belonging to free OH of carboxylic acid group at the chain end, 2900~2800 cm^{-1} for CH_2 repeat unit, 1722 cm^{-1} for ester (C=O) group and 1300~1000 cm^{-1} for C-O in the main chain.

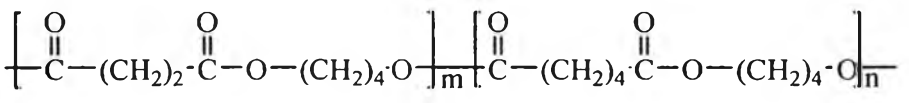

Figure 4.1 Chemical structure of PBSA.

Figure 4.3 (c) shows the infrared spectrum of poly(butylene adipate terephthalate) or PBAT (Ecoflex®) (as shown in Figure 4.2). Most of the peaks are similar to those of Bionolle® except an additional peak at 732 cm^{-1} referring to C=C aromatic.

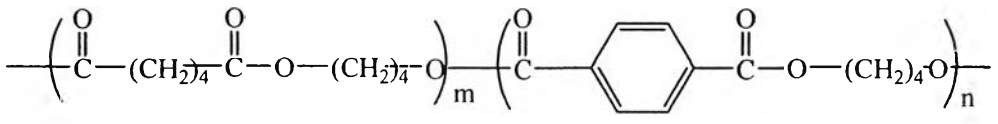

Figure 4.2 Chemical structure of PBAT.

For tapioca starch, the important peaks are 3409 cm^{-1} (OH), 2932 cm^{-1} (CH stretching), 1159~997 cm^{-1} (pyranose ring) (Figure 4.3 (d)).

The spectra of Terramac® (Figure 4.3 (e)), Lacea® (Figure 4.3 (f)), and Bioplast® (Figure 4.3 (g)) are found to be the combination of PLA (Figure 4.3 (a)) and PBAT (Figure 4.3 (c)), PLA and PBSA (Figure 4.3 (b)), and PBAT and starch (Figure 4.3 (d)), respectively.

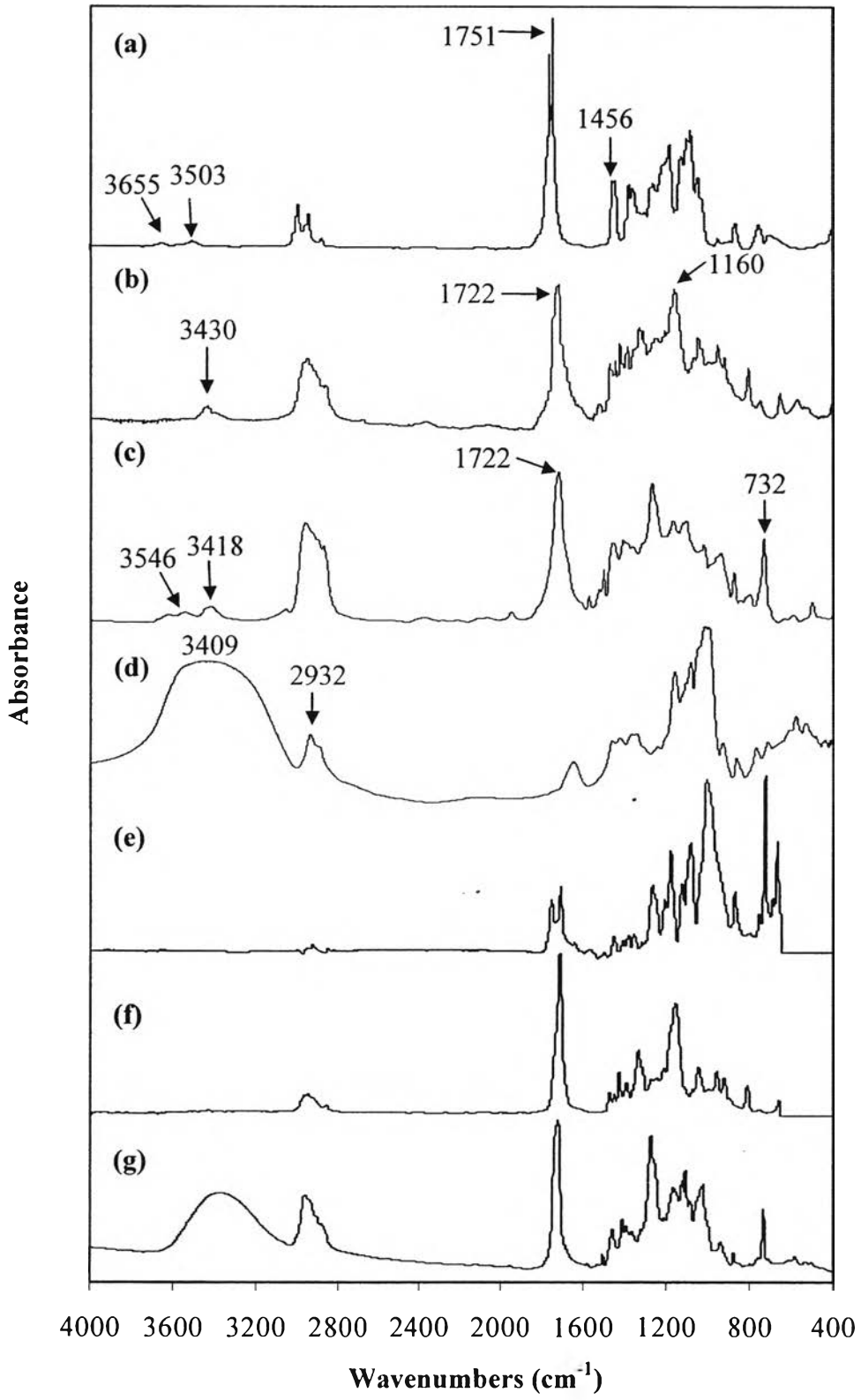

Figure 4.3 Infrared spectra of (a) PLA, (b) PBSA, (c) PBAT, (d) starch, (e) Terramac® , (f) Lacea® , and (g) Bioplast®.

4.1.2 Thermal Properties

DSC thermogram was applied to observe how much the energy needed in order to make the chain movement (glass transition temperature (T_g) and melting temperature (T_m)) in the heating step. Cold crystallization (T_c) was also observed. The cooling step was done to observe any crystallization (T_c).

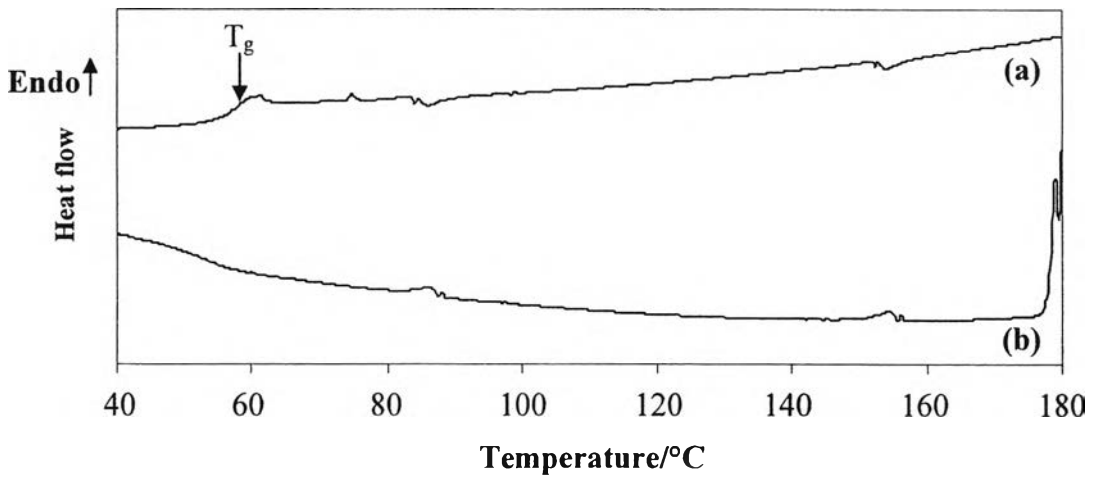

Figure 4.4 DSC thermogram of PLA NatureWorks® 4042D (a) heating step and (b) cooling step.

Figure 4.4 clearly shows T_g at 61°C. This indicates the glassy state of PLA at room temperature. The T_c and T_m are not observed in PLA.

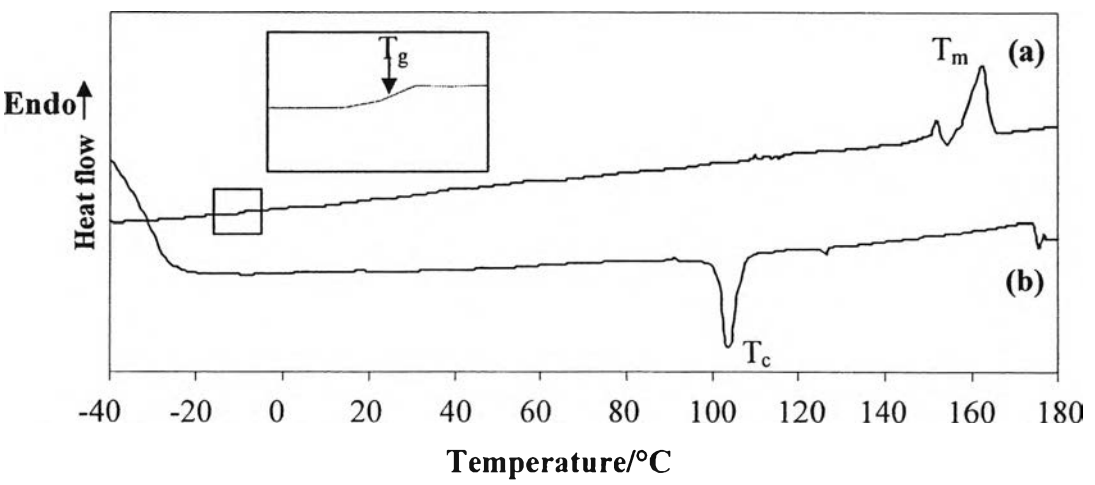

Figure 4.5 DSC thermogram of Terramac® (a) heating step and (b) cooling step.

Figure 4.5 shows the thermal properties of Terramac®. The T_g is at -9.94°C whereas T_c is at 103.67°C and T_m is at 162.17°C.

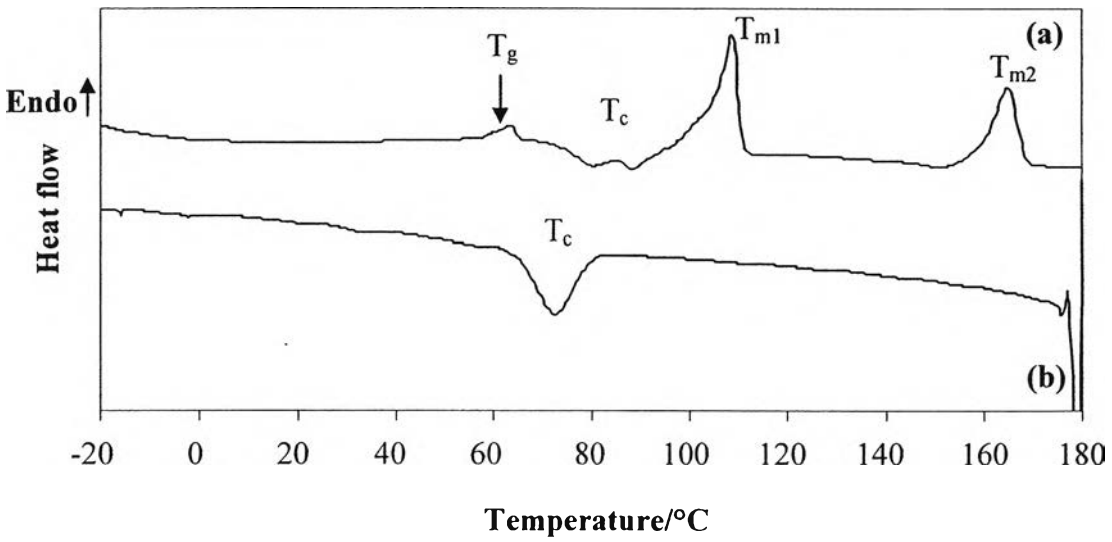

Figure 4.6 DSC thermogram of Lacea® (a) heating step and (b) cooling step.

Figure 4.6 shows the thermal properties of Lacea®. In the cooling step, the T_c is found at 72.33°C. In the heating step, T_g, cold crystallization temperature (T_c) and two endothermic peaks belonging to T_m are at 60, 88.5, 109.17 and 165°C, respectively. The blend between PLA and PBSA is immiscible as confirmed from the non-shifted T_g and two separated T_m. The T_m at 109.17°C is for PBSA and at 165°C for PLA.

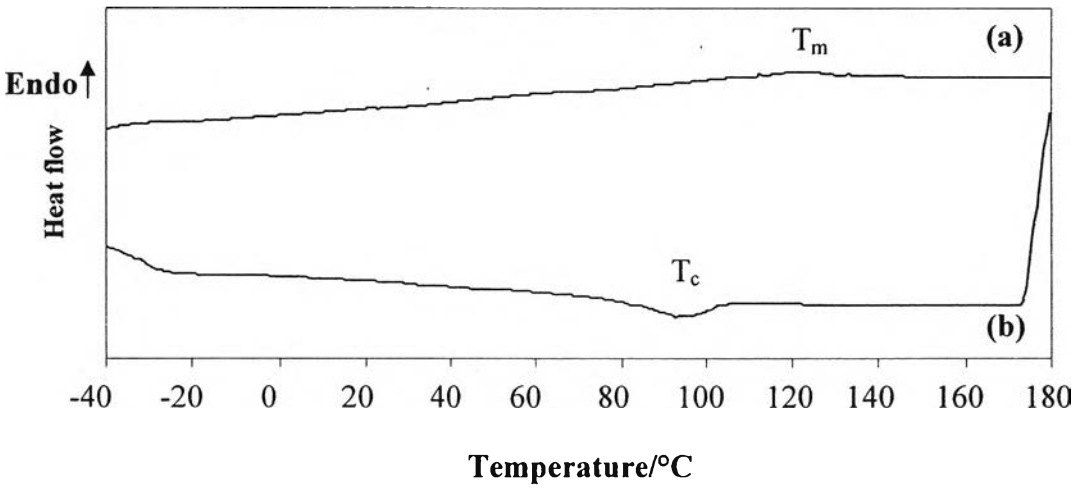

Figure 4.7 DSC thermogram of Bioplast® (a) heating step and (b) cooling step.

Figure 4.7 shows the thermal properties of Bioplast®. The DSC thermogram consists of exothermic broad peak at 93.83°C and endothermic peak at 120.83°C belonging to T_c and T_m, respectively. The T_g is not observed in DSC thermogram.

4.1.3 Spherulite Formation

In general, polarizing optical microscope is applied to observe the crystal morphology. In this study, the crystal morphology was observed at various temperatures. The optical micrograph of PLA (Figure 4.8 (a)) shows dark image. This implies the amorphous packing structure. However, for the commercial biodegradable plastic bags, Terramac® (Figure 4.8 (b)), Lacea® (Figure 4.8 (c)), and Bioplast® (Figure 4.8 (d)), the crystalline morphologies were observed even each was different in spherulitic appearances.

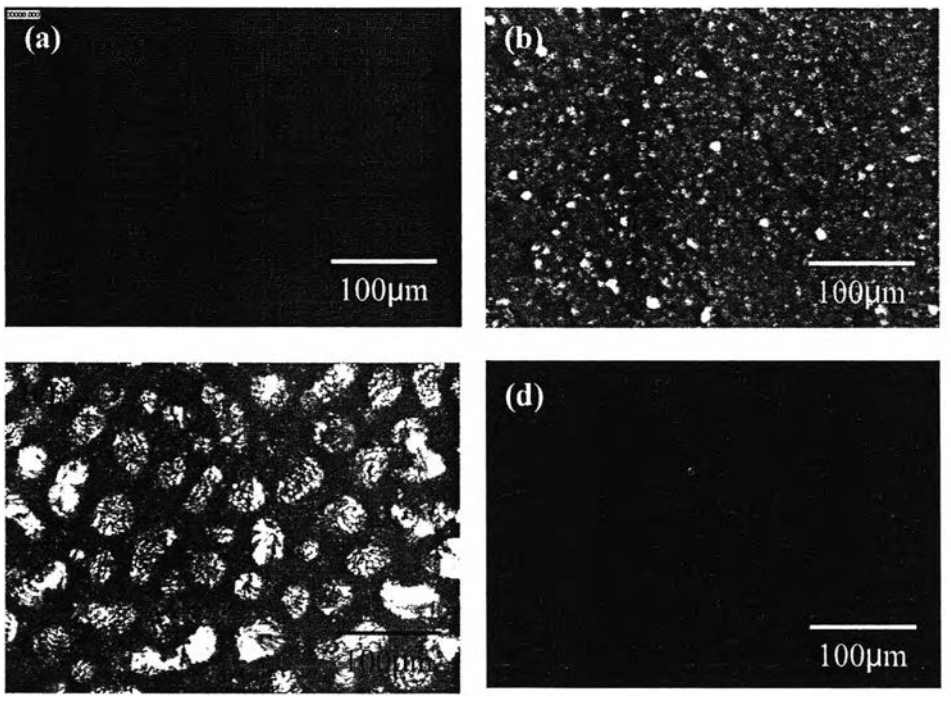

Figure 4.8 Optical Micrographs of (a) PLA, (b) Terramac®, (c) Lacea®, and (d) Bioplast®.

4.1.4 Morphological Observation

The morphologies of fractured surface of commercial biodegradable plastics bags were observed by SEM.

For Terramac® (Figure 4.9 (a)), the SEM photograph shows the homogeneous blend meaning that PLA and PBAT are miscible. For Lacea® (Figure 4.9 (b)), a little amount of small particles (~2 μm) was observed. No particles observed in case of Bioplast® (Figure 4.9 (c)). This means that the starch particles were destructured before blending with PBAT.

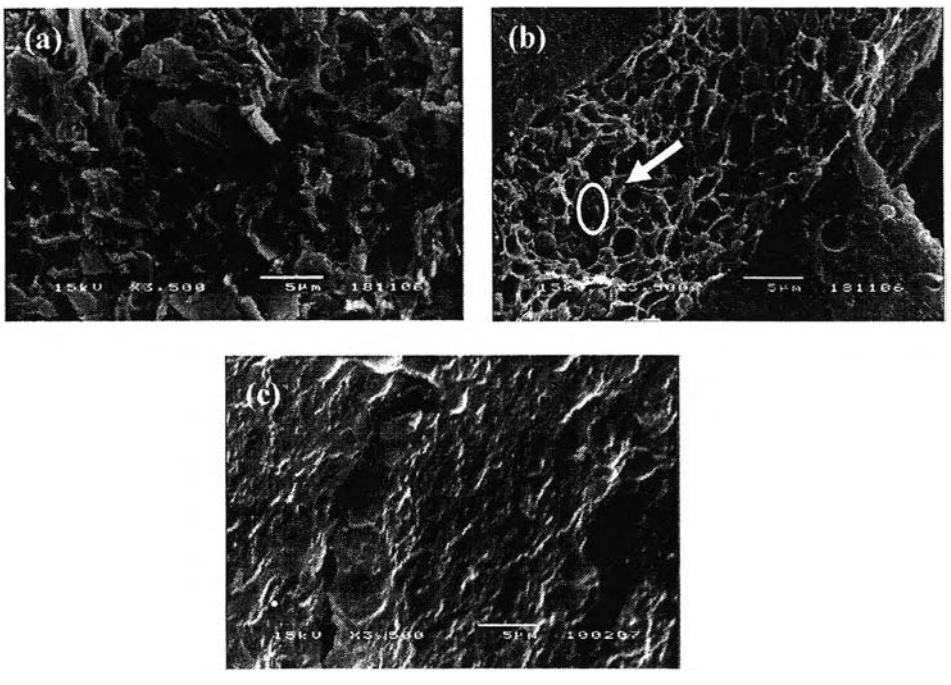

Figure 4.9 SEM photographs of (a) Terramac®, (b) Lacea®, and (c) Bioplast® with 3500x magnification.

4.2 Plasticization of PLA

Table 4.1 summarizes the T_g of pure PLA, pure PBSA and the blends consisting of PLA with various plasticizers obtaining from DSC. The T_g of PLA is 61°C which is much higher than room temperature leading to the brittleness of PLA. In order to overcome this problem, the addition of plasticizer is proposed. In our study, the T_g of PLA was slightly decreased from 61°C to 56.6°C and 55°C for **4** and **7** with the addition of PBSA into PLA/starch blend and PLA, respectively. This related to the fact that the T_g of PBSA is much lower than room temperature. When glycerol was added into PLA/PBSA/starch blend as in **5**, the T_g of PLA further shifts down for 0.5°C. However, in the presence of PEG 200, the T_g of PLA decreased significantly. This might be due to the short PEG chains penetrate and embed themselves between the PLA chains and initiate the mobility PLA-PEG matrixes. Here, PEG 200 is considered as an efficient plasticizer. However, based on the

positive list in producing biodegradable plastics, glycerol and PEG 200 can be added within 1 wt%. Although PEG is biodegradable (Frings, J. *et.al.*, 1992) its molecular weight is lower than 1,000 resulting in the adding amount as controlled by the positive list. Thus, PEG which has the molecular weight 6,000 and 20,000 were used instead of PEG 200 to observe the efficiency of plasticization. For PEG 6,000, **8**, the T_g of PLA was decreased to 50.4°C. For PEG 20,000, **9**, the T_g peak was not observed as it overlaps the T_m of PEG 20,000 at 62.5°C. We concluded that the optimum plasticizer for T_g reduction of PLA plastic product is PEG 6,000.

Table 4.1 T_g of PLA and the ones with various plasticizers

Sample	T_g (°C)
Pure PLA	61
Pure PBSA	<0
4	56.6
5	56.1
6	48.4
7	55
8	50.4
9	N/A

4.3 Nucleation of PLA

In order to find the effectiveness of nucleating agent for PLA, PLA with various nucleating agents were characterized by evaluating the T_c and the performance of crystallization using DSC and polarizing optical microscope, respectively.

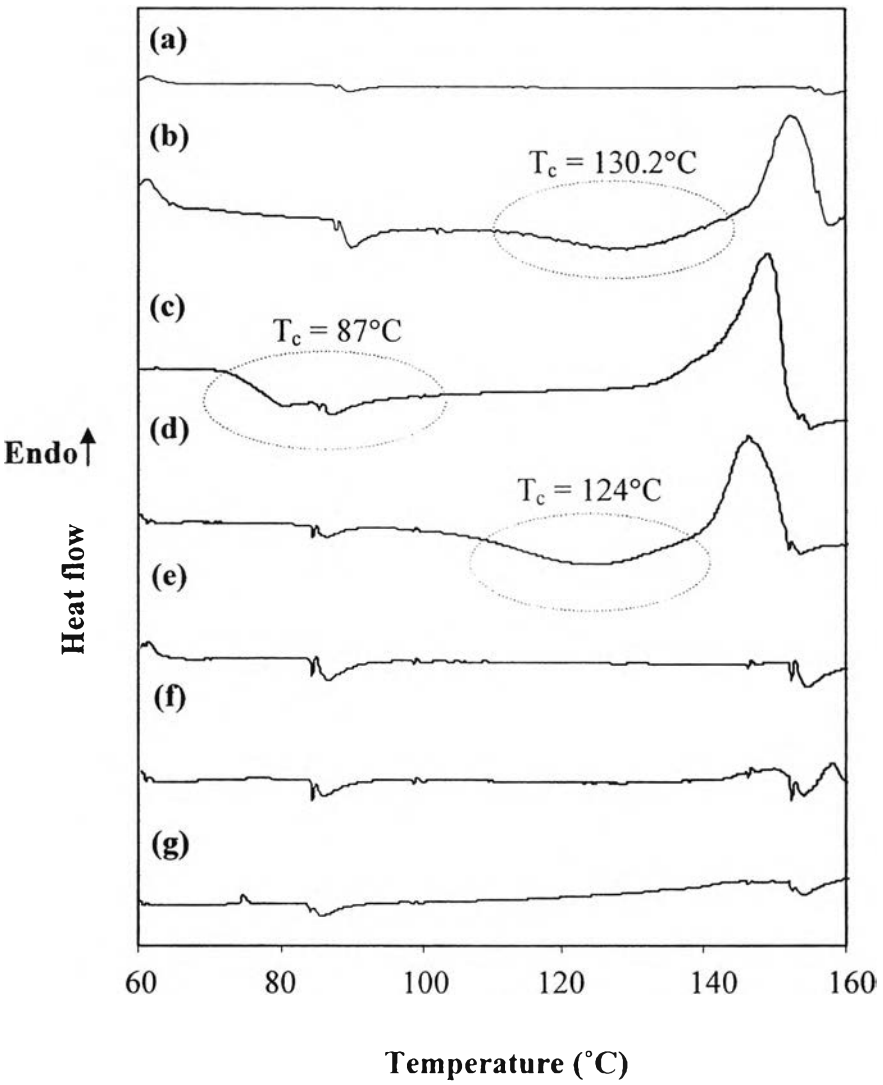

Figure 4.10 DSC thermograms of (a) PLA NatureWorks® 4042D, (b) **1**, (c) **8**, (d) **10**, (e) **11**, (f) **12**, and (g) **13**.

Table 4.2 T_c and T_m of PLA and PLA with various nucleating agents

Sample	T_c (°C)	T_m (°C)
Pure PLA	-	-
1	130.2	152.7
8	87	148
10	124	147
11	-	-
12	-	-
13	-	-

Table 4.2 shows the T_c and T_m of PLA and PLA with various nucleating agents. For pure PLA (Figure 4.10 (a)), no T_c or T_m peak is observed this might be related to the fact that PLA is amorphous. Here, it is expected that the nucleating agent induces the semicrystalline structure to PLA. As shown in Figure 4.10 (b) tapioca starch is not only functioned as a filler but also as a nucleating agent as identified from the T_c and T_m peaks in DSC thermograph. In the presence of PEG 6,000, T_c and T_m peaks of PLA appear at 87°C and 148°C, respectively (Figure 4.10 (c)). This implies that PEG 6,000 might be both plasticizer and nucleating agent. When 1% of talc (**10**), cloisite Na^+ (**11**), POM (**12**) or succinic acid (**13**) was incorporated into PLA, only **10** shows the T_c and T_m peaks at 124°C and 147°C respectively (Figure 4.9 (d)). This confirms that talc is a good candidate for nucleating agent.

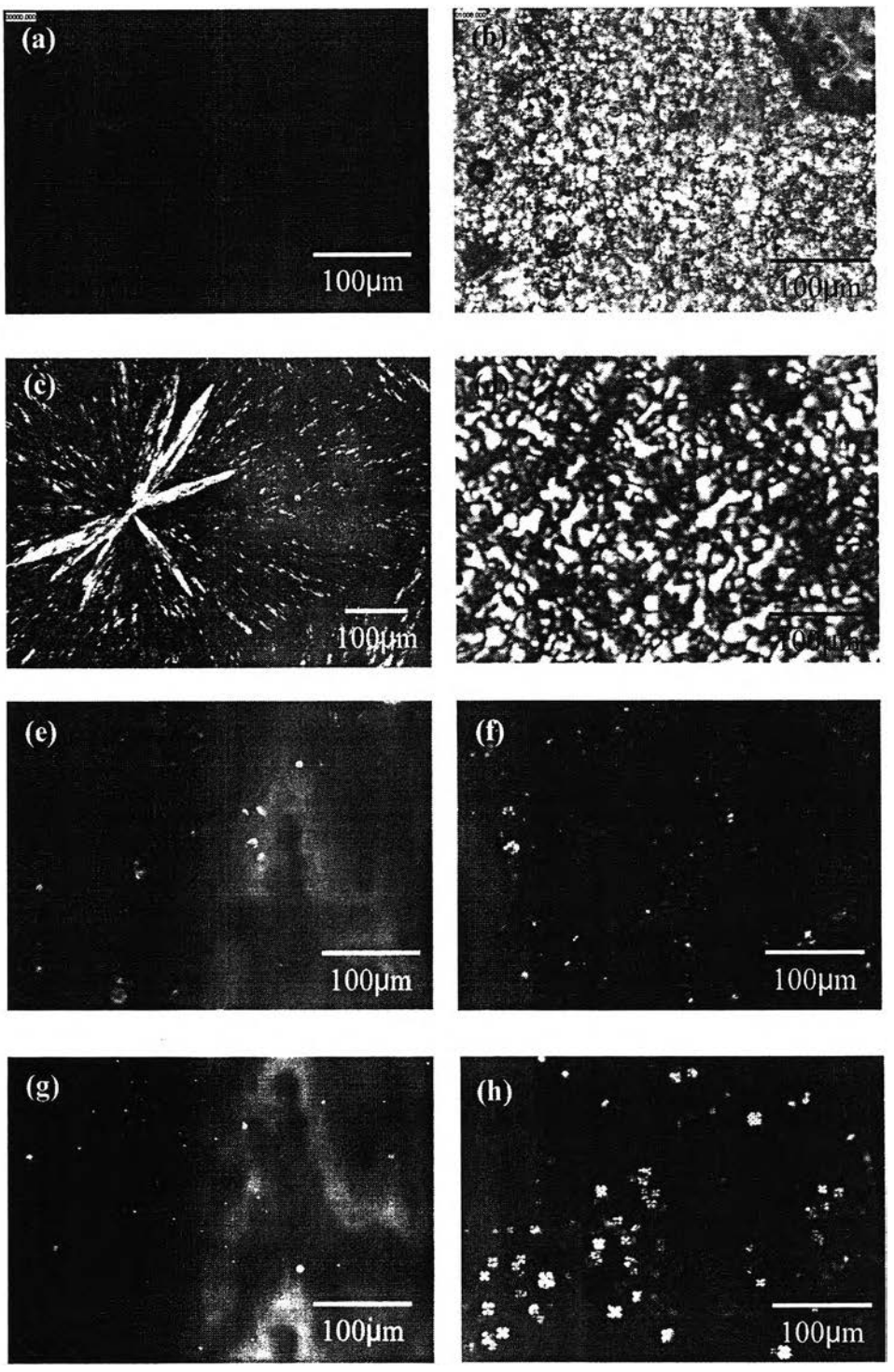

Figure 4.11 Optical micrographs of (a) PLA NatureWorks® 4042D, (b) **1**, (c) PEG 6,000, (d) **8**, (e) **10**, (f) **11**, (g) **12**, and (h) **13** at room temperature.

Figure 4.11 shows optical micrographs of PLA and PLA with various nucleating agents at room temperature. Because PLA is an amorphous polymer, the crystalline parts or white appearances are not observed (Figure 4.11 (a)). When tapioca starch was added into PLA, **1**, crystalline parts appear thoroughly (Figure 4.11 (b)) meaning that tapioca starch can be nucleating agent for PLA. Figure 4.11 (c) shows a large diameter of crystalline sphere of PEG 6,000. However, when PEG 6,000 was incorporated into PLA, **8**, the optical microscope (Figure 4.11 (d)) shows small crystalline spheres overall area. Thus, PEG 6,000 is a nucleating agent which induces a crystalline phase. For **10-13**, crystalline phases belonging to talc, cloisite Na^+, POM, and succinic acid, respectively, were observed in some particular area (Figure 4.11 (e)-(h)). However, considering the results above only talc can be concluded as an effective nucleating agent of PLA.

4.4 Compatibilization of PLA and Tapioca Starch Filler

As tapioca starch is cheap and available in Thailand, the use as an additive in PLA products is attractive. However, PLA and tapioca starch have difference in hydrophilicity, the compounding of two materials needs the compatibilizer. Compatibilizer which can bond or enhance the adhesion between two phases, was incorporated in order to achieve the miscibility.

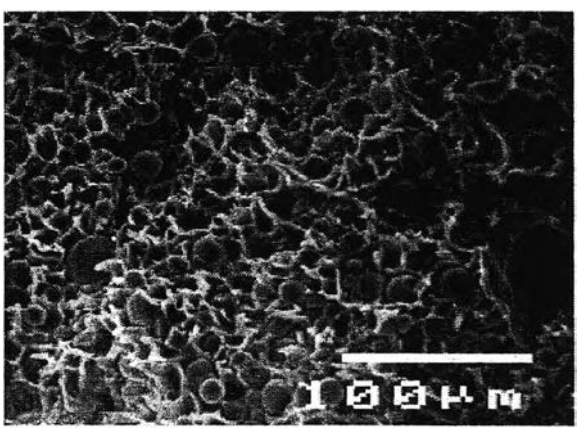

Figure 4.12 SEM photograph of **14** with 150x magnification.

From the SEM photograph of fractured surface of **14** (Figure 4.12), PLA forms the matrix and tapioca starch is dispersed. The fair dispersion of starch in the PLA matrix is identified.

For **1**, **2**, and **14** (Figure 4.13 (a), (b), and (g)), some area of starch particles connected with the matrix are observed. This indicated some extent of interaction between PLA and starch. For **3-5** and **15-16** (Figure 4.13 (c)-(e) and (h)-(i)), the thread-like connection or adhesion between tapioca starch particle and PLA matrix are observed. Maleic anhydride, 3-glycidoxypropyltrimethoxysilane, glycerol and MDI enhance the interfacial adhesion between two phases implying the possibility of the function in compatibility. For **6** (Figure 4.13 (f)), the compounding reveals the immiscibility of starch in PLA matrices.

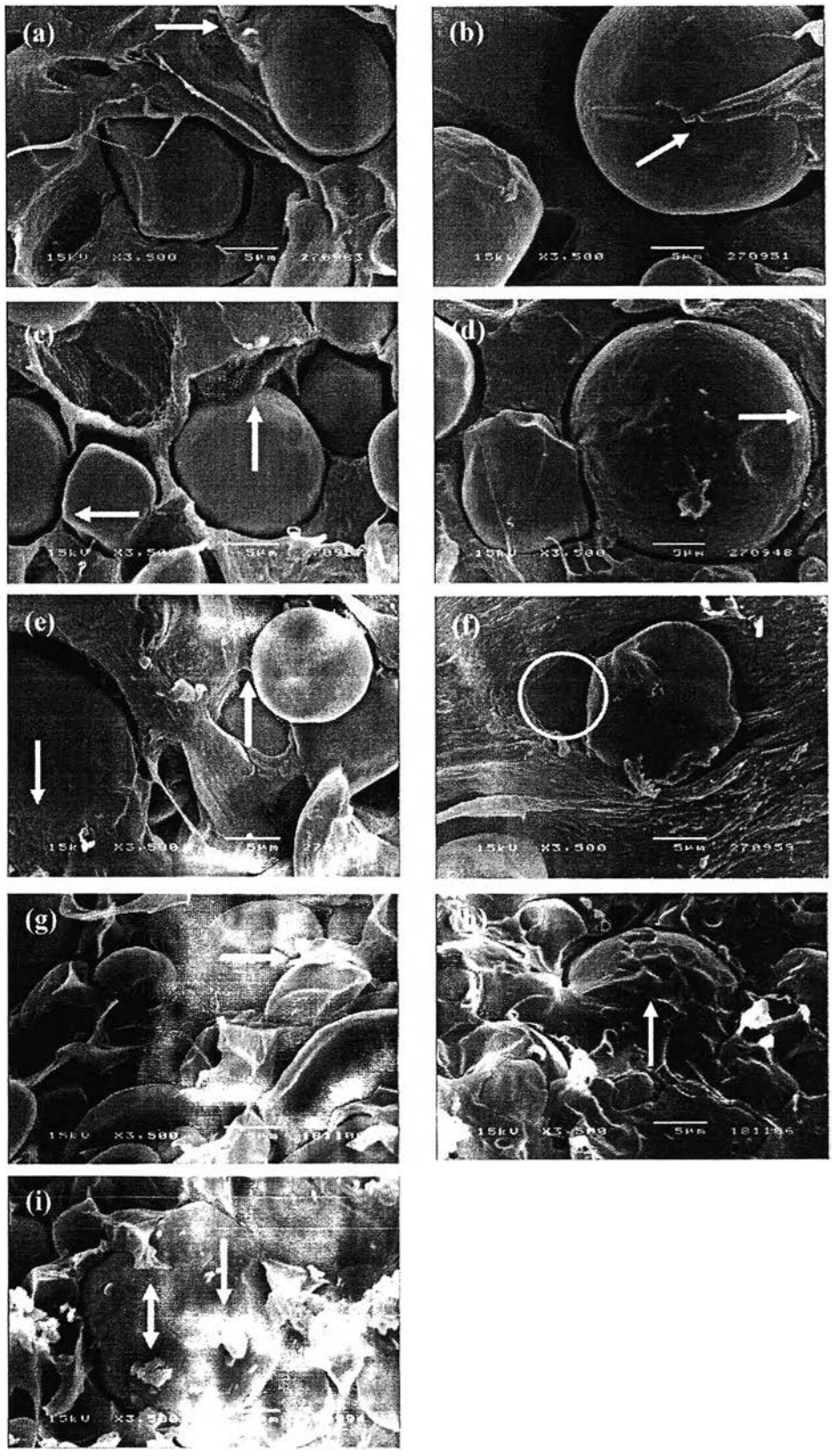

Figure 4.13 SEM photographs of (a) **1**, (b) **2**, (c) **3**, (d) **4**, (e) **5**, (f) **6**, (g) **14**, (h) **15**, and (i) **16,** with 3500x magnification, arrows indicate the adhesion between tapioca starch particle and PLA matrix and circle indicate the immiscibility of starch in PLA matrices.

MDI might be a good compatibilizer for PLA and starch blend as claimed in a USA patent (62211325). MDI gives the urethane linkage between the carboxyl and hydroxyl groups from PLA and starch (Wang H *et al.*, 2001), however, the toxicity of MDI has to be aware of. Table 4.3 shows the mechanical properties to evaluate the optimum compatibilizer.

Table 4.3 Mechanical properties of PLA/PBSA/starch blend with and without various compatibilizers

Sample	Compatibilizer	Young's Modulus (GPa)	Tensile Strength (MPa)	Elongation at Break (%)
2	-	1.11±0.18	18.27±1.69	5.06±0.59
3	Maleic anhydride	1.47±0.21	20.46±1.46	3.55±0.46
4	3-Glycidoxypropyl trimethoxysilane	1.15±0.26	23.58±2.64	5.89±2.02
5	Glycerol	1.04±0.09	18.44±1.95	4.77±0.74

Sample 4 shows the highest tensile strength and elongation at break. This implies that 3-glycidoxypropyltrimethoxysilane is effective in enhancing the interfacial adhesion between PLA matrix and tapioca starch particles. This also related to the hydroxyl and epoxy groups which are possible to bond with carboxyl or hydroxyl groups of PLA and starch.

4.5 Preliminary Studies of the Films

The films were preliminary studied by casting.

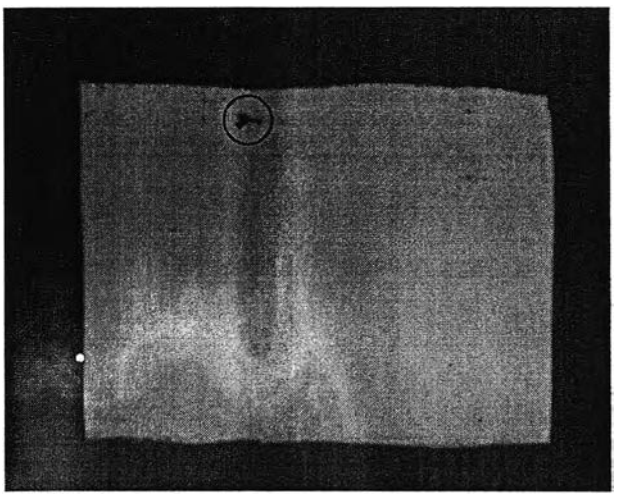

Figure 4.14 Film appearance of 17.

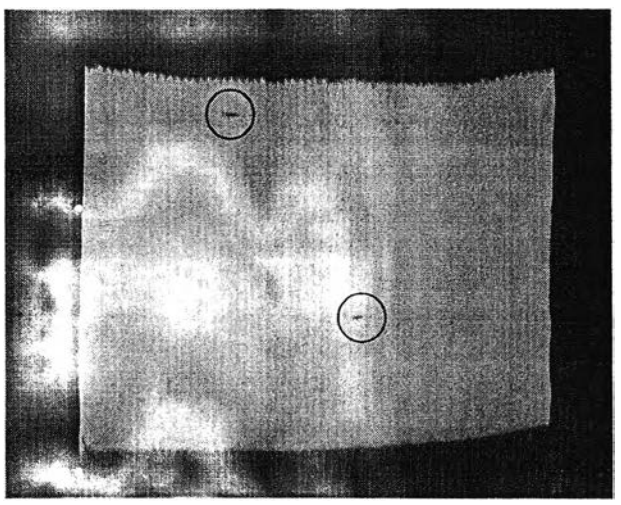

Figure 4.15 Film appearance of 18.

The films 17 and 18 are in the thickness of 0.4 mm. The pores are distributed implying the immiscibility os starch and PLA. The thermal properties of **17** were shown in Figure 4.16. The T_g strongly reduced from 61°C to 25.8°C. Moreover, T_c and T_m are observed at 90.86 °C and 150.53°C, respectively. The thermal properties of **18** were similar to that of **17** consisting of T_g at 26.4°C, T_c at

87.2°C, and T_m at 150.2°C (Figure 4.17), meaning that these compounds were semicrystalline structures.

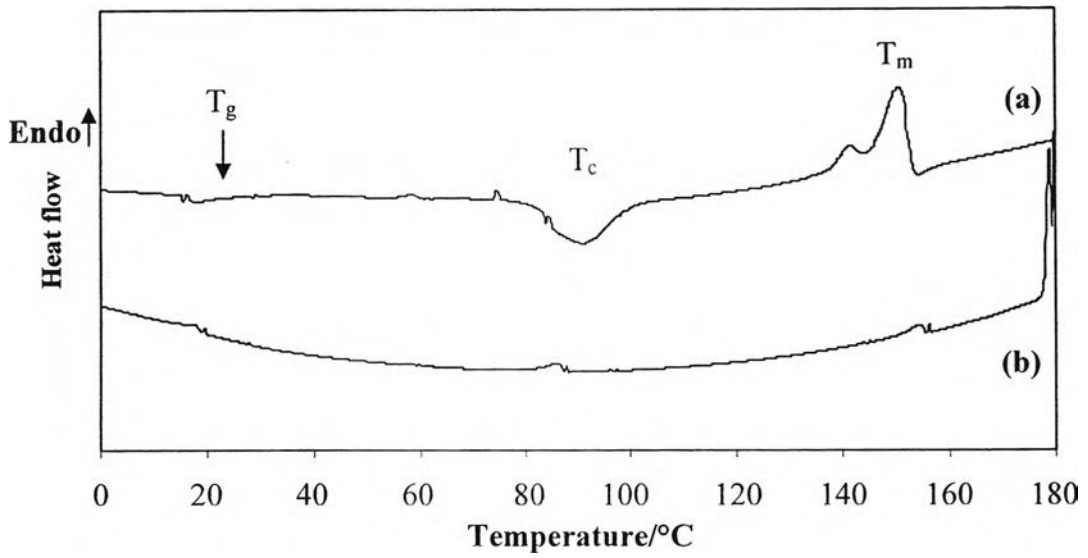

Figure 4.16 DSC thermogram of **17** (a) heating step and (b) cooling step.

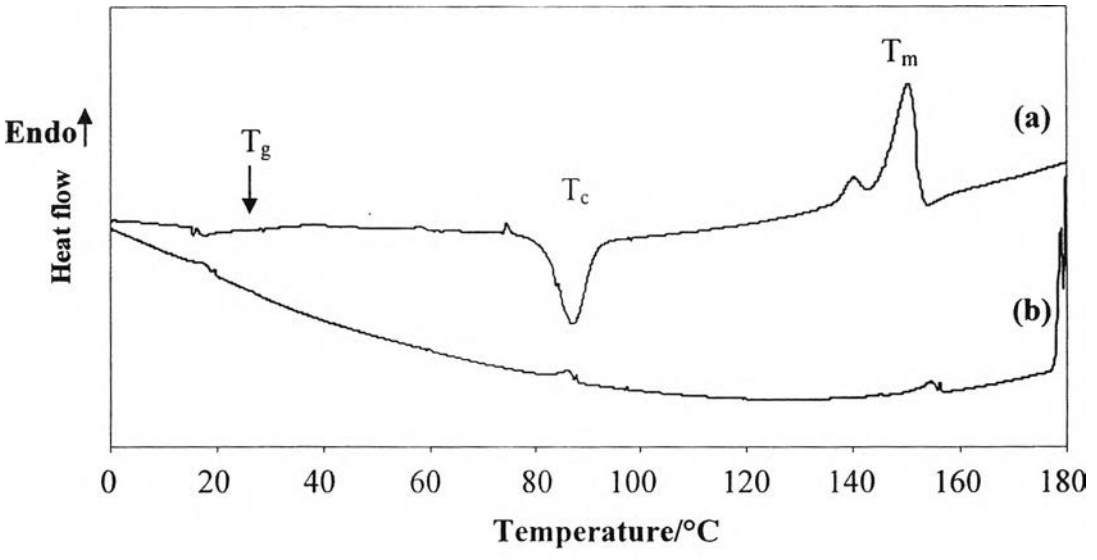

Figure 4.17 DSC thermogram of **18** (a) heating step and (b) cooling step.

The film **19** with the tapioca starch content 10%, was obtained by blown film extruder. The mechanical properties of **19** are shown in Table 4.4 comparing with that of pure PLA. The elongation at break increased strongly from 8.55% for

pure PLA to 41.89% for **19**. However, the young's modulus and tensile strength of **19** are lower than that of pure PLA.

Table 4.4 Mechanical properties of pure PLA and **19**

Sample	Young's Modulus (GPa)	Tensile Strength (MPa)	Elongation at Break (%)
Pure PLA	1.53±0.42	36.98±2.85	8.55±4.67
19	0.92±0.14	16.79±2.13	41.89±11.43

Figure 4.18 indicates the heating of **19** gives T_g, T_c and two endothermic peaks belonging to T_m at 20.45, 67.5, 52.5 and 146.33°C, respectively. In the cooling step, the T_c is found at 30.17°C and 69.5°C. The blend between PLA and PEG 6,000 is partial miscible because the T_m and T_c of PEG 6,000 are observed at 52.5 and 30.17°C, respectively. This may be due to an excess amount of PEG 6,000 in the blend.

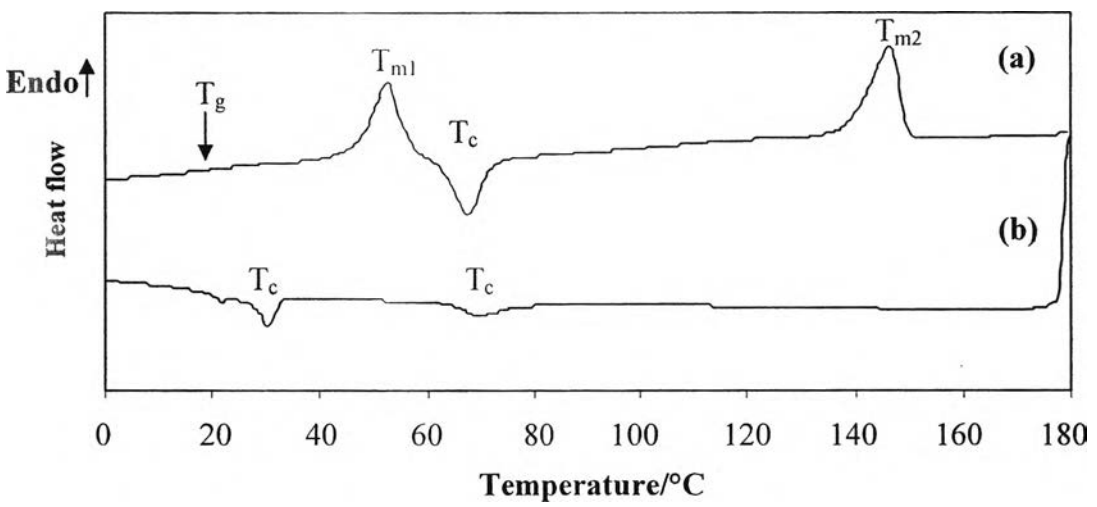

Figure 4.18 DSC thermogram of **19** (a) heating step and (b) cooling step.